Hindawi
Complexity
Volume 2018, Article ID 2563834, 12 pages
https://doi.org/10.1155/2018/2563834

Research Article

Decentralized Robust Saturated Control of Power Systems Using Reachable Sets

Hisham M. Soliman,[1] **Hassan A. Yousef**,[1] **Rashid Al-Abri**,[1] **and Khaled A. El-Metwally**[2]

[1]*Department of Electrical and Computer Engineering, Sultan Qaboos University, Muscat, Oman*
[2]*Electrical Engineering Department, Cairo University, Giza, Egypt*

Correspondence should be addressed to Hisham M. Soliman; hsoliman10@gmail.com

Received 11 February 2018; Revised 12 April 2018; Accepted 2 July 2018; Published 12 September 2018

Academic Editor: Arturo Buscarino

Electric power grids are highly nonlinear complex systems. This manuscript presents a novel approach to the stabilization of large power systems. The proposed control satisfied three constraints: decentralization, input saturation imposed in practice, and robustness against load changes. The large power system is decomposed into subsystems, for each a decentralized controller is designed. The effect of the rest of the system on each subsystem is considered as an external disturbance and represented in norm-bounded form. A new approach to solve this problem is proposed in the present paper. The approach is based on the method of invariant ellipsoids, and the tool of linear matrix inequalities (LMI) is utilized to solve the resulting optimization problem. Control of multimachine power system is studied using the proposed control. Comparison with other techniques is also given.

1. Introduction

Power system stability studies are important to insure reliable and continuous service to the consumers. There are three types of stability studies: voltage stability, frequency stability, and angle stability (transient and small disturbance).

Small disturbance stability studies low frequency electromechanical oscillations that arise at synchronous generators after perturbations (load and topology variations). Automatic voltage regulators (AVR) are used to adjust the terminal voltage of generators. A large value in the AVR gain may result in negative damping leading to an oscillatory behavior and loss of stability. These oscillations can cause blackouts and great loss of national economy if they are not suitably damped [1]. The oscillations can be classified as follows: (i) local (when a generator swings against the rest of the system at 1.0 to 2.0 Hz) and (ii) inter-rea (when two coherent groups of generators swing against each other at 1 Hz or less) [1, 2].

Power system stabilizers (PSS) are controllers installed on synchronous generators to damp power oscillations through the excitation channel. The main function of PSS is to modulate the field voltage of generators to provide an additional damping torque (in phase with rotor speed deviations) [1]. The types of PSS can be an output feedback or state feedback.

The classical output feedback structure of PSS is composed of single- or double-lead blocks to provide the required oscillation damping. The most common input signals to the PSS are speed deviation and electrical power [2].

Conventional power system stabilizers (CPSS) are output feedback controllers allocated to damp local oscillations, and through proper tuning, they can provide a suitable damping for interarea modes associated to generators on which they are fitted. The tuning process of CPSS is a difficult task due to load variation. In other words, if the CPSS is tuned at one operating point, there is no guarantee that it works well at another.

There are several techniques to handle the PSS tuning problem. These techniques can be classified into four groups: (i) classical control and pole placement, (ii) robust control, (iii) artificial intelligence, and (iv) optimization approaches to fine tune most of the abovementioned methods.

The methodologies based on classical control, for example, frequency response methods, are well established, and they are the most commonly used in the industry. Nonetheless, they consist of a sequential design in which one PSS is designed at a time (using a single-machine infinite bus equivalent system). In addition, the tuning procedure is performed for a single operating condition, requiring a trial-and-error approach if robustness is to be considered [3].

There are many design methods based on robust control theory to provide PSS which is robust against system load variations [4]. Model uncertainty due to load variations can be represented in different forms: interval plant, norm-bounded, and polytopic. The uncertainty modeled as an interval plant is found in [5]. The Kharitonov theorem is used to design robust PSS for interval plants as given in [5]. Comparison between the μ-synthesis and the H_∞ loop-shaping approaches is found in [6]. However, such approach requires many trials and errors to find suitable weighting transfer functions. Power system uncertainty represented by a linear parameter varying (LPV) model and gain-scheduled control is applied as presented in [7]. The PSS can also be designed using linear quadratic regulator (LQR). To achieve a good dynamic performance in terms of desired settling time and damping ratio, the closed-loop poles must be placed in a desired region for all admissible load variations. Lyapunov-based matrix inequalities (linear matrix inequalities (LMI) and bilinear matrix inequalities (BMI)) are used to achieve a regional pole placement. Plant and controller uncertainties represented by a norm-bounded model and a resilient PSS design achieving regional pole placement are given in [8].

Intelligence techniques such as artificial neural networks (ANNs) and fuzzy logic (FL) are used to design PSS. These methods suffer from the long training time of ANNs and the extensive previous knowledge of the system behavior required for the FL application [9].

Optimization techniques are another alternative to the PSS design. The PSS is tuned to optimize performance indices in terms of the damping ratio and the dominant poles. One of the great advantages of using these techniques is that the tuning procedure is automatically made. In addition, once an optimization method fails, it can be restarted with new initial conditions [10, 11]. There are two main groups of the optimization techniques: (i) search direction-based methods (that use derivatives or not) and (ii) metaheuristics methods.

The search direction-based methods provide fast convergence. However, it can stick in a local minimum, and also it is sensitive to the initial solution guess. For nonconvex optimization problems (such as the PSS design [10]), the global solution may not be achieved by these methods.

Metaheuristics methods are probabilistic and derivative-free techniques which seek global solutions at a reasonable computational burden. Most metaheuristics approaches are population-based methods that use a set of solutions (individuals) to solve an optimization problem. The individual solutions are simple; however, their collective effect produce a surprising result. These methods are suitable for global optimization since it explores the whole search space. So, stucking in a local minimum is very remote. Nonetheless, they tend to present a slow convergence. Some applications of metaheuristics for conventional PSS tuning are: genetic algorithms, ant colony optimization, bat algorithm [11], cuckoo search algorithm [12], gravitational search [13], particle swarm optimization [14], bacteria foraging optimization [15], grey wolf optimization [16], and water cycle algorithm [17].

The amplifier, as an actuator, in the exciter circuit suffers from saturation limits. Practically, the imposed saturation limits are considered as ($\pm$0.1 pu) [18]. Violation of these limits can lead to degradation of system performance and even instability. The impact of such effects has received little attention during the last decade [19]. The PSS of [19] achieves regional pole placement with saturated input for a certain operating range. For wider range than that in [19], the LMIs may not converge to a solution. This problem is solved by dividing the whole range of operation into subregions, for each a saturated robust pole placer can be easily found. A 2-dimensional fuzzy logic control is then trained to switch between the subregions to cover the whole region [20]. On the other hand, there are many saturated control techniques available in the control literature, for example, [21, 22] and the references therein. One of these approaches is the positive invariance which is based on avoiding the control constraint, that is, to prevent saturation in the closed-loop [22]. Several other saturated control design techniques such as L_1 optimization, the small and high gain, and model predictive control have been presented in [23–25].

In addition to the control input constraint, large interconnected power systems represent another challenge in terms of stabilization and control design. Due to the high dimensionality of large power systems, the above approaches require the system order reduction to reduce the computational burden and the controllers' order. Also, these methodologies may fail to converge.

Although the controller presented in [19] achieves regional pole placement with saturated PSS, it has centralized structure and relies on the state variables of all other machines in the system. Decentralized control uses the local states of its own subsystem. It needs no communication network to transmit the states of the large system to a hub computer, and hence, the delay and packet dropouts are avoided. Decentralization is also cost-effective. Different decentralized PSS design techniques are presented [26–29]. In [26], a PSS design scheme based on robust decentralized output feedback sliding mode control technique is presented. Fixed parameter-decentralized power system stabilizers (PSSs) are proposed in [27] where the local information available at each machine in the multimachine environment is used to tune the parameters of PSS. A multimachine power system is approximated to a single-machine infinite bus, and then conventional design technique is used to design decentralized PSS [28]. Reference [29] represents power system uncertainty due to load variations as a linear parameter varying (LPV) system. For the resulting system, the gain scheduling method is applied to design a decentralized PSS. The designed controller automatically adjusts its parameters depending on the scheduling variables to coordinate with change of operating conditions. The controller achieves high performance but at expense of controller complexity. These techniques did not consider the saturation limits of the control signal nor the parameter uncertainty involved in the power system due to different loading.

In this work, robust decentralized power system stabilizer with saturated inputs is proposed. In the proposed control scheme, the multimachine power system is decomposed into several subsystems. With regard to each subsystem, the effect of the rest of the system is considered as an external bounded disturbance. Rejection of bounded disturbance is considered as a difficult problem and has been traditionally tackled using the L_1-optimization technique which results in higher order controller [23, 24]. The method of invariant sets is used for rejecting the bounded disturbance optimally [30]. In this paper, the invariant ellipsoids are used as the invariant sets to reject bounded disturbance by minimizing the size of the invariant ellipsoids of the dynamic system [31]. Doing that, the problem of decentralized control is reduced to equivalent conditions in the form of linear matrix inequalities (LMI) with the advantage of using the $L\infty$-optimization.

The main contributions of the paper are as follows: (1) a simple new design of state feedback PSS is presented. (2) The proposed design achieves three constraints: decentralization, robustness, and no control limit violation. (3) The design is based on a simple LMI sufficient condition.

The paper is organized as follows. A mathematical model of a multimachine power system and problem statement is presented in Section 2. In Section 3, the use of the invariant ellipsoid technique for disturbance rejection is outlined. This technique is essential in the design of decentralized PSS. Section 4 presents the problem solution using the LMI method and stability of the closed-loop system under the proposed control scheme. Simulation results for a multimachine power system are provided in Section 5 to validate the effectiveness of the proposed decentralized controller. Comparison between the proposed controller and the H_∞ control as a disturbance rejection approach is presented in Section 6. The paper is concluded in Section 7.

1.1. Notations. Throughout this paper, the notation $\mathbb{R}^m$ is the set of vectors of $m \times 1$ dimension, $\mathbb{R}^{r\times q}$ is the set of real matrices of dimension $r \times q$, and $(.)'$ denotes the transpose of a vector or a matrix. For a matrix $\mathbf{P}$, $\mathbf{P} > 0$ (<0) means that $\mathbf{P}$ is a symmetric positive (negative) definite matrix. Also, $(^*)$ in a matrix means the symmetric part. Similarly, $(\mathbf{M} + \mathbf{N} + *)$ means $(\mathbf{M} + \mathbf{N} + \mathbf{M}' + \mathbf{N}')$. Finally, $\mathbf{0}$ and $\mathbf{I}$ denote the zero matrix and the identity matrix, respectively.

2. Mathematical Modeling and Problem Formulation

In matrix form, the system dynamics [1] of a large power system consist of n generators that can be described by the overall model.

$$\dot{x} = \mathbf{A}\mathbf{x} + \mathbf{B}\mathbf{u}, \tag{1}$$

where $\mathbf{x} = [\mathbf{x}_1, \dots, \mathbf{x}_n]' \in \mathfrak{R}^{4n\times 1}$ is the composite state vector. The components of the element $\mathbf{x}_i$ of the state vector are defined as $x_i = [\Delta\delta_i \, \Delta\omega_i \, \Delta E'_{qi} \, \Delta E_{fi}]' \in \mathfrak{R}^{4\times 1}$ where $\Delta\delta_i$ is the relative rotor angle changes with respect to the reference generator, $\Delta\omega_i$ is the rotor speed deviation, $\Delta E'_{qi}$ is the deviation in the quadrature axis transient voltage, and ΔE_{fi} is the deviations in the field voltage. Note that the state, $\Delta E'_{qi}$ is not measurable. This state can be replaced by a measurable one, $\Delta \mathbf{P}_e$ (machine output power) using the transformation given in [32].

To formulate the problem in a way suitable to design a decentralized control, the overall system (1) is decomposed into n subsystems. The model for the ith generator takes the form

$$\dot{x}_l = \mathbf{A}_{ix_i} + \mathbf{B}_i\mathbf{u}_i + \sum_{j=1,\, j\neq i}^{n} \mathbf{A}_{ij}\mathbf{x}_j, \quad i = 1, \dots, n, \tag{2}$$

where $\mathbf{x}_i = [\Delta\delta_i \, \Delta\omega_i \, \Delta E'_{\mathrm{q}} \, \Delta E_{\mathrm{f}i}]'$ and the terms $\sum_{j=1, j\neq i}^{n} \mathbf{A}_{ij}\mathbf{x}_j$ represent the interconnection with other generators. This term is considered in the sequel as external disturbance to the ith subsystem.

The control objective is stated as follows. For each machine system described in (2), design a decentralized saturated control law in the form

$$\mathbf{u}_i = \mathbf{K}_i\mathbf{x}_i, \quad -\mu < \mathbf{u}_i < +\mu, \mu > 0. \tag{3}$$

The controller must be also robust against load changes. To this effect, we have to answer two questions. Firstly, how to deal with the uncertainty associated with the power system model? And secondly, how to design a decentralized control in the presence of the interconnection terms? In the next section, we give some mathematical preliminaries to deal with these two concerns.

3. Mathematical Preliminaries and the State-Invariant Ellipsoid Method

The approach of invariant ellipsoids has been used for disturbance rejection in control system theory [31]. A design of state feedback control while attenuating the effect of an arbitrarily bounded disturbance can be achieved by minimizing the size of the invariant ellipsoids defined for a given dynamic system. As a result, the control design problem is reduced to equivalent conditions in the form of linear matrix inequalities (LMI).

Consider the linear time-invariant (LTI) system.

$$\dot{x} = \mathbf{A}\mathbf{x} + \mathbf{B}\mathbf{u} + \mathbf{D}\mathbf{w}, \tag{4}$$

where $\mathbf{x}(t)$, $\mathbf{u}(t)$, and $\mathbf{w}$ are the system state, input, and disturbance vectors, respectively. System (4) is subject to the constraint that the disturbance $\mathbf{w}(t)$ is bounded as

$$\|\mathbf{w}(t)\| \leq 1, \quad \forall t \geq 0. \tag{5}$$

Note that no other constraints are imposed on $\mathbf{w}(t)$; that is, they are not assumed to be random or harmonic and so on. We assume that the matrix pair $(\mathbf{A}, \mathbf{B})$ is controllable.

The proposed approach is based on the reachable sets. The reachable set is defined as the set that contains the state trajectories for systems subject to external disturbances [30]. Since the reachable set is extremely difficult to calculate mathematically, it is approximated by a bounding ellipsoid, termed the invariant ellipsoid. The meaning of invariant is explained later. Approximating the reachable sets by an ellipsoid facilitates the controller design of a system with disturbances. Specifically, a smaller ellipsoidal bound of a reachable set for linear systems with constrained inputs allows a larger control gain, consequently improving system performance. The invariant ellipsoid technique is a challenging alternative to L_1 approach because the last one is based on the assumption $\mathbf{x}(0) = 0$, and nonzero initial conditions can cause serious troubles. In contrast, invariant ellipsoids automatically cover nonzero initial conditions.

Consider an ellipsoid E centered at the origin and given by

$$E = \left\{ \mathbf{x} : \mathbf{x}'\mathbf{P}^{-1}\mathbf{x} \le 1 \right\}, \quad \mathbf{P} > 0, \tag{6}$$

where $\mathbf{P}$ is a symmetric matrix termed as the matrix of the ellipsoid. This ellipsoid bounds and approximates the reachable sets of the system (4) subject to the constraint (5).

The ellipsoid E is called a state invariant if, for any initial state $\mathbf{x}(0)$ starting inside E, the trajectory $\mathbf{x}(t)$ remains inside the ellipsoid for the future time $t > 0$. It is shown in [31] that an invariant ellipsoid is also attracting for LTI systems. In other words, if the initial state $\mathbf{x}(0)$ starts outside the ellipsoid, the trajectory $\mathbf{x}(t)$, $t > 0$ is attracted to it.

The invariant ellipsoid reflects the effect of external disturbance on the trajectories of the dynamic system. To minimize this effect, an objective function in terms of the ellipsoid matrix $f(\mathbf{P})$ has to be formulated first. Due to its linearity, the trace function

$$f(\mathbf{P}) = \mathrm{tr}(\mathbf{P}) \tag{7}$$

that corresponds to the sum of the squares of the semiaxes of the state-invariant ellipsoid of the original system is selected as the objective function, where tr(.) means the trace of (.). Note that there are different measures of size for ellipsoids: $f_1(\mathbf{P})$ = tr $\mathbf{P}$ (associated with the sum of squared semiaxes), $f_2(\mathbf{P}) = \mathrm{Det}\ \mathbf{P}$, $f_3 = -\ln(\det \mathbf{P}^{-1})$ (associated with the maximization of the volume of $E(\mathbf{P})$), $f_4(\mathbf{P})$ = (spectral matrix norm), or f_5 = minimal eigenvalue (associated with the radius of the inscribed ball), and so on. In this paper, we adopt the trace function because it retains the semidefinite program (SDP) structure of the problem (optimization of a linear function subject to LMI constraints), which is then solvable by means of widely available MATLAB-based software. Also, standard geometric properties of the ellipsoids are considered to come up with a convex programming formulation, easy to solve, of the constrained stabilization problem.

Suppose the control objective is to design a state feedback.

$$\mathbf{u} = \mathbf{K}\mathbf{x}. \tag{8}$$

The following theorem gives the necessary and sufficient conditions for the existence of the matrix $\mathbf{P}$ such that the ellipsoid (6) is state-invariant.

Theorem 1 (see [31]). *The ellipsoid E of the form (6) is state-invariant for the system (4) with bounded disturbance (5) if and only if for some fixed $\alpha > 0$, the matrix $\mathbf{P}$ satisfies the following LMI:*

$$\mathbf{P}\mathbf{A}_c' + \mathbf{A}_c\mathbf{P} + \alpha\mathbf{P} + \frac{1}{\alpha}\mathbf{D}\mathbf{D}' \le 0. \tag{9}$$

Or equivalently,

$$\begin{bmatrix} \mathbf{A}_c\mathbf{P} + * & \mathbf{D} \\ * & -\alpha\mathbf{I} \end{bmatrix} \le 0, \tag{10}$$

where $\mathbf{A}_c = \mathbf{A} + \mathbf{B}\mathbf{K}$ is the closed-loop matrix.

Now, if the control signal is constrained by

$$\|\mathbf{u}(t)\| \le \mu. \tag{11}$$

This constraint on the control can be transformed to an equivalent LMI using the following lemma.

Lemma 1 (see [31]). *For the controllable system (4) with bounded disturbance (5) and state feedback control (8), constraint (11) is equivalent to satisfying the LMI*

$$\begin{bmatrix} \mathbf{P} & * \\ \mathbf{Y} & \mu^2\mathbf{I} \end{bmatrix} \ge 0, \quad \mathbf{P} > 0, \tag{12}$$

for the matrices $\mathbf{P}$ and $\mathbf{Y}$ where $\mathbf{Y} = \mathbf{K}\mathbf{P}$. The proof of this lemma is detailed in [31] and will be omitted here.

Now, Theorem 1 and Lemma 1 are combined in the following theorem.

Theorem 2 (see [31]). *Consider the controllable system (4) subject to the bounded external disturbance (5). Then the problem of designing a state feedback controller (8) with the constraint (12) that optimally rejects the disturbance is equivalent to the following constrained optimization problem for the matrices $\mathbf{P}$ and $\mathbf{Y}$. The controller gain matrix $\mathbf{K}$ is calculated as then given by $\mathbf{K} = \mathbf{Y}\mathbf{P}$. Note that constraint (14) guarantees the system stability with disturbance, whereas (15) represents the control constraint. Moreover, the ellipsoid E defined in (6) bounds the reachable sets of the system (4) with disturbance and control constraints. The matrix inequality (14) is nonlinear in the scalar $\alpha > 0$. For a fixed α, (14) becomes a linear matrix inequality (LMI). The problem, thus, reduces to a one-dimensional minimization. The minimization problem is solved using linear search optimization. In other words, α is iteratively updated (using linear search) such that the objective function (13) is minimized.*

$$\min_{\alpha,\mathbf{P},\mathbf{Y}} \quad \mathrm{tr}(\mathbf{P}), \tag{13}$$

subject to the constraints,

$$(\mathbf{AP}+\mathbf{BY}+*)+\alpha\mathbf{P}+\frac{1}{\alpha}\mathbf{DD}'\le 0, \quad \alpha>0, \tag{14}$$

$$\begin{bmatrix} \mathbf{P} & * \\ \mathbf{Y} & \mu^2\mathbf{I} \end{bmatrix} \ge 0, \quad \mathbf{P}>0. \tag{15}$$

4. Stability of the Closed-Loop

The above result is extended to the decentralized control problem of large power systems as follows. Consider the ith subsystem defined in (2). The dynamic equation can be cast as

$$\dot{x}_i = \mathbf{A}_i\mathbf{x}_i + \mathbf{B}_i\mathbf{u}_i + \mathbf{D}_i\mathbf{x}, \quad i=1,\dots,n, \tag{16}$$

where the interaction of the global system on the ith subsystem is considered as a disturbance given by

$$\mathbf{D}_i = [\mathbf{A}_{i1}, \mathbf{A}_{i2}, \dots, \mathbf{0}_{ii}, \dots, \mathbf{A}_{in}], \tag{17}$$

and the vector $\mathbf{x}$ represents the state vector of the composite global system. The vector $\mathbf{x}$ is considered as an input disturbance. Note that this paper studies the stability of power systems, that is, small-disturbance (signal) stability [1]. Therefore, the condition $\|\mathbf{x}\|\le 1$ is assumed. Note that even for severe disturbances, $\|\mathbf{x}\|$ can normalize to 1 by using a new disturbance matrix (e.g., if $\|\mathbf{x}\| = 1.5\,\mathrm{pu}$, it can be normalized to 1 by selecting $\mathbf{D}_{\mathrm{new}} = 1.5\mathbf{D}_{\mathrm{old}}$).

Changes in power system operation and loads result in system uncertainties which are reflected in the system model as follows:

$$\dot{x}_i = (\mathbf{A}_i + \Delta\mathbf{A}_i)\mathbf{x}_i + \mathbf{B}_i\mathbf{u}_i + (\mathbf{D}_i + \Delta\mathbf{D}_i)\mathbf{x}, \quad i=1,\dots,n, \tag{18}$$

where the uncertainties $\Delta\mathbf{A}_i$ and $\Delta\mathbf{D}_i$ are represented by a norm-bounded form as follows:

$$\Delta\mathbf{A}_i = \mathbf{M}_i\Delta_i(t)\mathbf{N}_i, \quad \|\Delta_i(t)\|\le 1, \tag{19}$$

$$\Delta\mathbf{D}_i = \mathbf{F}_i\Delta_i(t)\mathbf{H}_i, \quad \|\Delta_i(t)\|\le 1. \tag{20}$$

Note that casting the uncertainty in the norm-bounded form can be easily obtained using the singular value decomposition as given in [33].

The following theorem establishes the main design result for subsystem i. It tackles the ellipsoidal bound of a reachable set for the uncertain system (18) with constraints (3), (5), (19), and (20).

Theorem 3. *Consider the family of uncertain controllable subsystems described by (18) subject to the bounded external disturbance (17) and (20). Then, this family of subsystems is asymptotically stabilizable by a decentralized robust controller* $\mathbf{u}_i = \mathbf{K}_i\mathbf{x}_i$, $i=1,\dots,n$ *with input constraint (11). The local controller optimally rejects the disturbances if there exist matrices* $\mathbf{P}_i(\alpha_i)>0$ *and* $\mathbf{Y}_i(\alpha_i)$ *solutions of the following optimization problem*

$$\min_{\alpha,\mathbf{P},\mathbf{Y}} \quad \mathrm{tr}(\mathbf{P}), \tag{21}$$

subject to the constraints,

$$\begin{bmatrix} (\mathbf{A}_i\mathbf{P}_i+\mathbf{B}_i\mathbf{Y}_i+*)+\alpha_i\mathbf{P}_i+\varepsilon\mathbf{M}_i\mathbf{M}_i'+\rho_i\mathbf{F}_i\mathbf{F}_i' & * & * & * \\ \mathbf{D}_i' & -\alpha_i\mathbf{I} & * & * \\ \mathbf{H}_i\mathbf{P}_i & \mathbf{0} & -\varepsilon_i\mathbf{I} & * \\ \mathbf{0} & \mathbf{H}_i & \mathbf{0} & -\rho_i\mathbf{F}_i \end{bmatrix} < 0, \tag{22}$$

$$\begin{bmatrix} \mathbf{P} & * \\ \mathbf{Y} & \mu^2\mathbf{I} \end{bmatrix} \ge 0, \quad \mathbf{P}>0, \tag{23}$$

where $\mathbf{P}_i>0$ *and* $\mathbf{Y}_i$ *are functions of* α_i. *Moreover, the local gain matrix is given by* $\mathbf{K}_i = \mathbf{Y}_i\mathbf{P}_i^{-1}$.

Proof. Extension of Theorem 1 to the ith uncertain subsystem (18) with external admissible disturbance is stable if and only if the following LMI is satisfied.

$$\begin{bmatrix} (\{\mathbf{A}_i+\Delta\mathbf{A}_i\}\mathbf{P}_i+\mathbf{B}_i\mathbf{Y}_i+*)+\alpha_i\mathbf{P}_i & \mathbf{D}_i+\Delta\mathbf{D}_i \\ * & -\alpha_i\mathbf{I} \end{bmatrix} < 0, \tag{24}$$

applying the fact $\mathbf{\Psi}\Delta(t)\mathbf{\Phi} + * < \varepsilon\mathbf{\Psi}\mathbf{\Psi}' + \varepsilon^{-1}\mathbf{\Phi}\mathbf{\Phi}'$, $\varepsilon>0$ [34] to (19) and (20) to eliminate the uncertainty matrices in (24). The constant matrices $\mathbf{\Phi}$ and $\mathbf{\Psi}$ are of appropriate dimensions. This will result in the following.

$$\begin{aligned} &\begin{bmatrix} (\mathbf{A}_i\mathbf{P}_i+\mathbf{B}_i\mathbf{Y}_i+*)+\alpha_i\mathbf{P}_i & \mathbf{D}_i \\ * & -\alpha_i\mathbf{I} \end{bmatrix} \\ &+\varepsilon_i\begin{bmatrix}\mathbf{M}_i\\0\end{bmatrix}\begin{bmatrix}\mathbf{M}_i\\0\end{bmatrix}' + \varepsilon_i^{-1}\begin{bmatrix}\mathbf{N}_i\mathbf{P}_i\\0\end{bmatrix}'\begin{bmatrix}\mathbf{N}_i\mathbf{P}_i\\0\end{bmatrix} \\ &+\rho_i\begin{bmatrix}\mathbf{F}_i\\0\end{bmatrix}\begin{bmatrix}\mathbf{F}_i\\0\end{bmatrix}' + \rho_i^{-1}\begin{bmatrix}0\\\mathbf{H}_i'\end{bmatrix}\begin{bmatrix}\mathbf{F}_i\\\mathbf{H}_i'\end{bmatrix} < 0, \quad \varepsilon_i, \rho_i > 0. \end{aligned} \tag{25}$$

The nonlinear matrix (25) can be linearized (i.e., the form (22)) using the following Schur complement:

$$\mathbf{X} - \mathbf{YZ}^{-1}\mathbf{Y}' < 0 ? \begin{bmatrix}\mathbf{X} & \mathbf{Y} \\ * & \mathbf{Z}\end{bmatrix}, \quad \mathbf{Z}<0. \tag{26}$$

To prove stability of the global system with decentralized control, consider the scalar Lyapunov function.

$$V(t) = \sum_{i=1}^{n} V_i(t). \tag{27}$$

The stability of each subsystem $V_i(t)>0, \dot{V}_i(t)<0$ is satisfied if (22) is satisfied; hence with (27), the global system is also stable.

Note that the uncertainty in the input matrix $\mathbf{B}_i$ can be considered by putting the uncertainty in the norm-bounded

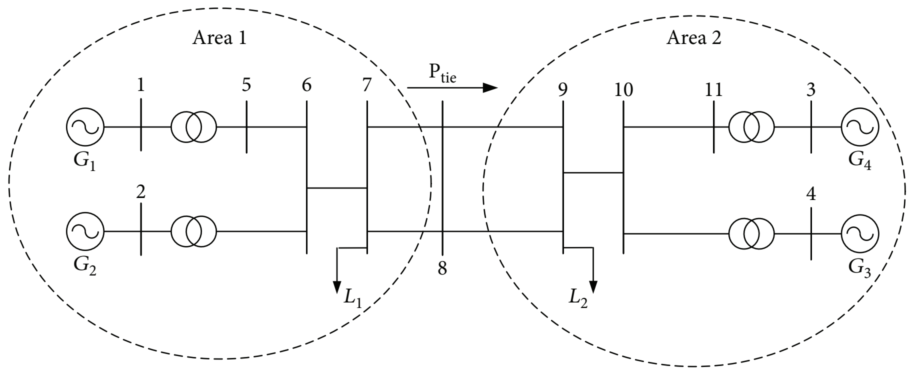

Figure 1: Two-area four-machine test power system.

form $\Delta\mathbf{B}_i = \mathbf{M}_{\mathbf{B},i}\Delta_{\mathbf{B},i}\mathbf{N}_{\mathbf{B},i}$, $\|\Delta_{\mathbf{B},i}\| \leq 1$. The above theorem can then be easily extended to include this case.

5. Simulation Example

The proposed design is applied to a multimachine power system. The benchmark four-machine 11-bus two-area test power system is shown in Figure 1. The two-area four-machine test power system shown in Figure 1 proposed in [1] is utilized in this study because it is accepted in the literature as a tool to study the interarea mode of oscillations. Further, this system is available as a MATLAB/SIMULINK demo program. The test system consists of two symmetrical areas linked together by two 230 kV lines of 220 km length. It is specifically designed in [1] to study low-frequency electromechanical oscillations in large interconnected power systems. Each area is equipped with two identical round rotor generators rated 20 KV/900 MVA. The synchronous machines have identical parameters except for the inertias which are $\mathbf{M}_1 = 13$ s and $\mathbf{M}_2 = 12.35$ s. Thermal plants have identical speed regulators equipped with fast static exciter with a gain of 200. The loads are represented as constant impedances and spilt between the two areas. The full parameters of a single unit are given in [1]. In the example system, generator number 4 is chosen as the slack bus. Since the interarea mode is strongly affected by the amount of the tie line power, three operating conditions are considered for the test system [19]:

Case 1 (the base case (tie-line power = 415 MW)).

Case 2 (20% decrease in tie-line power (334 MW)).

Case 3 (20% increase in tie-line power (502 MW)).

The interarea modes for Cases 1, 2, and 3 are, respectively, $0.0888 \pm j2.2585$, $0.1255 \pm j1.8179$, and $0.0444 \pm j2.4977$; the damping ratios are -0.0392, -0.0688, and -0.0177.

The system without PSSs achieves negative damping for the three test points. The three operating points of the system considered for generator numbers 1, 2, and 3 are given in [19]. Model (18) and the associated norm-bounded uncertainties (19) and (20) for the system are given in the appendix. All generators are equipped with the same regulator.

Solving the LMI's given in Theorem 3, the proposed decentralized controller is given by

$$\mathbf{K} = \text{Block diag}\,[\mathbf{K}_1, \mathbf{K}_2, \mathbf{K}_3], \tag{28}$$

where

$$\begin{aligned}\mathbf{K}_1 &= [\,0.1241 \quad 55.6 \quad -0.2928 \quad -0.0003\,],\\ \mathbf{K}_2 &= [\,0.0909 \quad 40.4149 \quad -0.2571 \quad -0.0005\,],\\ \mathbf{K}_3 &= [\,-0.0603 \quad 55.6431 \quad -0.6302 \quad -0.0043\,].\end{aligned} \tag{29}$$

The resulting controller is decentralized or local as it uses local states only from the generator on which it is installed. Local PSSs have three basic advantages. First, they are effective in damping local modes. Second, no communication network is needed to transfer data to a centralized controller; thus, they are cost-effective. Third, communication time delays are avoided.

The proposed controller is tested for a large disturbance, stimulated by a three-phase short-circuit taking place at the bus of generator number 1, cleared at $t = 0$. For heavy (502 MW) power transferred from area number 1 to area number 2, the rotor angle of generator numbers 1, 2, and 3 are shown in Figure 2. The control signals are shown in Figure 3 for such fault. It is evident that the proposed decentralized controller enhances the system stability at large tie line. The proposed control signals are indeed do not violate the limits ± 0.1 pu as depicted in Figure 3.

It is worth mentioning that u_1 starts near its upper limit (+0.1), as compared with u_2 and u_3, because the cleared fault occurs at the terminal of G_1. So, G_1 is much disturbed as compared with G_2 and G_3.

Low-frequency interarea oscillations (0.1–0.8 Hz) are detrimental to the goals of maximum power transfer and optimal power flow. Figure 2 shows the effectiveness of the proposed PSS added to the automatic voltage regulator in damping the interarea oscillations. This is achieved without violating the control limit (Figure 3). Other methods to damp interarea oscillations are found in [35–37].

Note that the power system model is linear time-invariant but with uncertainty. While it is not intended to be implemented, it is used to synthesize a linear controller. The success of the proposed PSS in stabilizing the original nonlinear system follows from the Lyapunov indirect

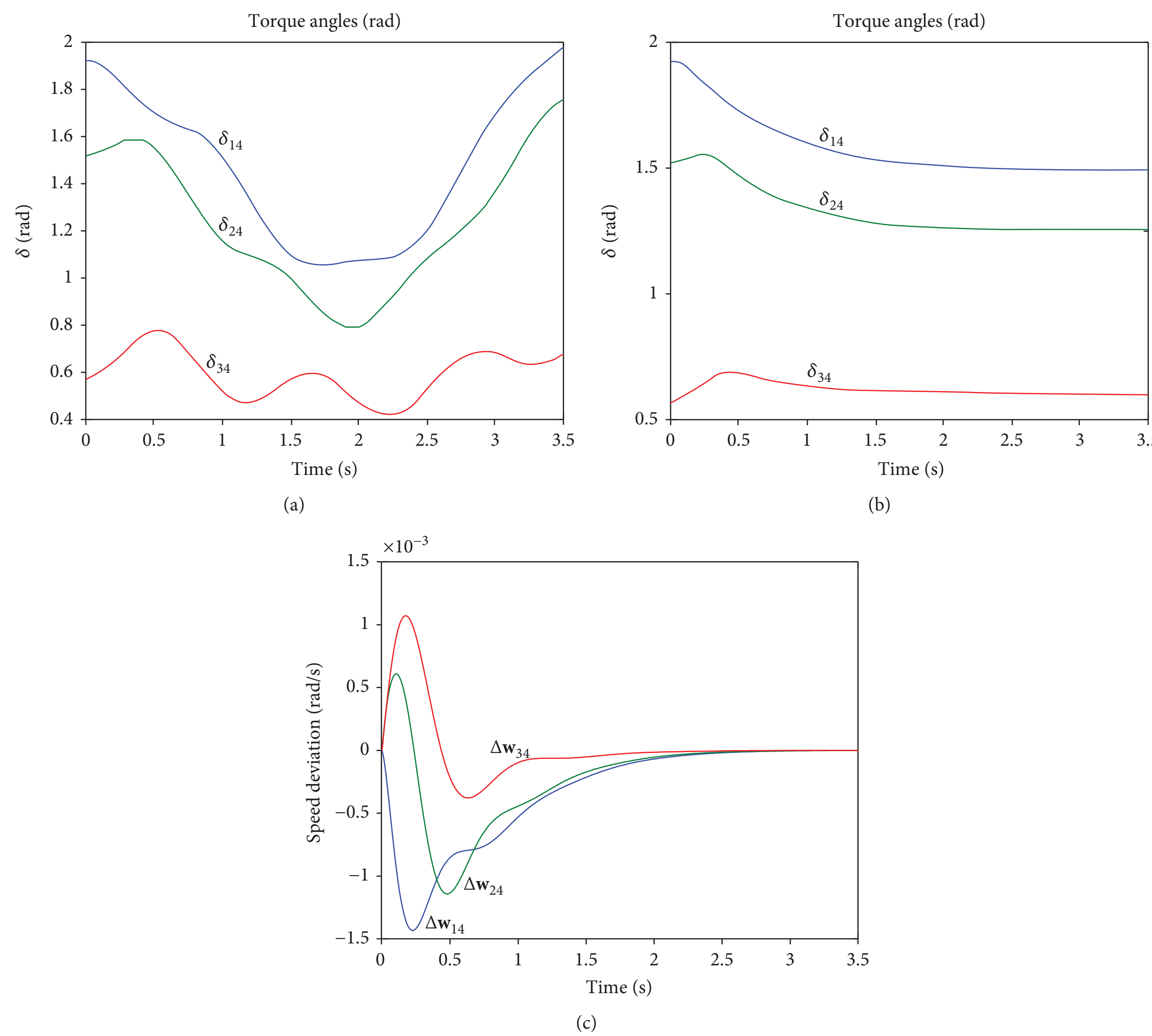

FIGURE 2: Generators' dynamics: (a) rotor angle without controller, (b) rotor angle with the proposed controller, and (c) speed deviation with the proposed controller.

theorem. According to that theorem, the behavior of the original nonlinear system is similar to its linearized approximation provided that none of the eigenvalues lies on the imaginary axis.

6. Comparison with Decentralized H_∞ Control

The H_∞ control can be used as a disturbance rejection approach [34]. Therefore, in this section, the proposed decentralized controller is compared to the H_∞ decentralized control technique. First, we give a summary of this approach.

Consider the following system without uncertainty.

$$
\begin{aligned}
\dot{x} &= \mathbf{A}\mathbf{x} + \mathbf{B}\mathbf{u} + \mathbf{D}\mathbf{w}, \\
\mathbf{z} &= \mathbf{C}_1\mathbf{x}, \\
\mathbf{y} &= \mathbf{C}_2\mathbf{x},
\end{aligned}
\tag{30}
$$

where $\mathbf{w}, \mathbf{z} \in \Re^q$, and $\mathbf{y} \in \Re^l$ are the disturbance, output to be regulated, and measured output, respectively. The H_∞ control problem is to find a state feedback controller in the form $\mathbf{u} = \mathbf{K}\mathbf{x}$ such that the closed-loop system is quadratically stable [34] and the effect of disturbance on the regulated output is minimized. This means that $\|T_{\mathbf{wz}}\|_\infty \le \gamma$ where $T_{\mathbf{wz}}$ is the transfer function from $\mathbf{w}$ to $\mathbf{z}$. The solution to this problem is the solution to the following matrix inequalities:

$$
\begin{bmatrix}
(\mathbf{A}\mathbf{X} + \mathbf{B}\mathbf{Y} + *) & * & * \\
\mathbf{D}' & -\mathbf{I} & * \\
\mathbf{C}_1\mathbf{X} & 0 & -\gamma^2\mathbf{I}
\end{bmatrix}, \quad \mathbf{X} = \mathbf{X}' > 0.
\tag{31}
$$

The H_∞ controller is given by $\mathbf{K} = \mathbf{Y}\mathbf{X}^{-1}$.

To design an H_∞ decentralized control, the original global system (4) with $\mathbf{A} = \{\mathbf{A}_{ij}\}$, $i, j = 1, \ldots, n$, is

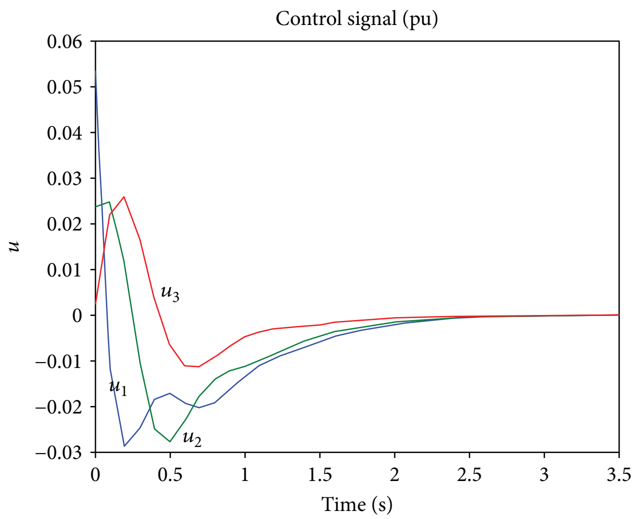

FIGURE 3: The control signal for each generator.

decomposed into a block diagonal and off-diagonal parts as follows:

$$\dot{x} = (\mathbf{A}_{\mathrm{d}} + \mathbf{A}_{\mathrm{off}})\mathbf{x} + \mathbf{B}\mathbf{u}, \quad \mathbf{z} = \mathbf{C}_1\mathbf{x}, \quad \mathbf{y} = \mathbf{C}_2\mathbf{x}, \tag{32}$$

where

$$\mathbf{A}_{\mathrm{d}} = \text{block diag}\,[\mathbf{A}_{11}, \mathbf{A}_{22}, \dots, \mathbf{A}_{\mathrm{nn}}],$$
$$\mathbf{A}_{\mathrm{off}} = \begin{bmatrix} 0 & \mathbf{A}_{12} & \cdots & \mathbf{A}_{1n} \\ \mathbf{A}_{21} & 0 & & \mathbf{A}_{2n} \\ \vdots & & \ddots & \vdots \\ \mathbf{A}_{n1} & \cdots & \mathbf{A}_{n,n-1} & 0 \end{bmatrix}, \tag{33}$$
$$\mathbf{B} = \text{block diag}\,[\mathbf{B}_1, \mathbf{B}_2, \dots, \mathbf{B}_n],$$

and the matrices $\mathbf{C}_1$ and $\mathbf{C}_2$ are selected as unity.

Considering the interconnection effect $(\mathbf{A}_{\mathrm{off}}\mathbf{x})$ as a disturbance designated by $\mathbf{Dw}$, we get

$$\dot{x} = \mathbf{A}_{\mathrm{d}}\mathbf{x} + \mathbf{B}\mathbf{u} + \mathbf{D}\mathbf{w}. \tag{34}$$

The system with uncertainty due to load variation is then given by

$$\dot{x} = (\mathbf{A} + \Delta\mathbf{A})\mathbf{x} + \mathbf{B}\mathbf{u} + (\mathbf{D} + \Delta\mathbf{D})\mathbf{w}, \quad \mathbf{z} = \mathbf{C}_1\mathbf{x}, \quad \mathbf{y} = \mathbf{C}_2\mathbf{x}, \tag{35}$$

where the uncertainty is represented by the norm-bounded form

$$\Delta\mathbf{A} = \mathbf{M}\Delta_1(t)\mathbf{N}, \quad \Delta\mathbf{D} = \mathbf{F}\Delta_2(t)\mathbf{H}, \quad \|\Delta_!\| < 1, \quad \|\Delta_2\| < 1. \tag{36}$$

The decentralized H_∞ control $\mathbf{u} = \mathbf{Kx}$ with $\mathbf{K} = \text{block diag}\,[\mathbf{K}_1, \mathbf{K}_2, \dots, \mathbf{K}_n]$ can be determined using the next theorem.

Theorem 4. *Consider the uncertain controllable system described by (35) and (36). Then, this system is asymptotically stabilizable by the decentralized robust controller $\mathbf{u}_i = \mathbf{K}_i\mathbf{x}_i$ if there is a feasible solution to the following optimization problem.*

$$\begin{aligned} \min \quad & \gamma \\ \text{subject to} \quad & \mathbf{X} = \mathbf{X}' > 0, \\ & \varepsilon > 0, \\ & \rho > 0, \end{aligned}$$
$$\begin{bmatrix} \left(\mathbf{AP} + \mathbf{BY} + *\varepsilon\mathbf{MM}' + \rho\mathbf{FF}'\right) & * & * & * & * \\ \mathbf{D}' & -\mathbf{I} & * & * & * \\ \mathbf{C}_1\mathbf{X} & 0 & -\gamma^2\mathbf{I} & * & * \\ \mathbf{NX} & 0 & 0 & -\varepsilon\mathbf{I} & * \\ 0 & \mathbf{H} & 0 & 0 & -\rho\mathbf{I} \end{bmatrix} < 0. \tag{37}$$

The controller gain matrix is determined from $\mathbf{K} = \mathbf{YX}^{-1}$. Note that in (37), $\mathbf{X}$ and $\mathbf{Y}$ are block diagonal matrices.

Proof. The proof is straightforward from (35), and using the Schur's inequality, so we omit the details. The result stated in the above theorem is applied to the previous simulation example. The decentralized H_∞ controller gain matrices are found as

$$\begin{aligned} \mathbf{K}_1 &= [-0.13587 \quad 5.8264 \quad -0.78451 \quad -0.010179], \\ \mathbf{K}_2 &= [-0.017814 \quad 0.38667 \quad 0.52462 \quad -.010037], \\ \mathbf{K}_3 &= [0.059358 \quad 0.06913 \quad 0.48116 \quad -0.010023]. \end{aligned} \tag{38}$$

The best degree of stability achieved is 0.17715. Simulation results of the rotor angles for the same disturbance and loading conditions mentioned in Section 5 are depicted in Figure 4. It is clear that the proposed controller is much faster in damping the system oscillations than the H_∞ controller. Moreover, the proposed control is obtained by solving small-dimension LMIs of each subsystem whereas the decentralized H_∞ control solves large LMIs having the dimension of the global system.

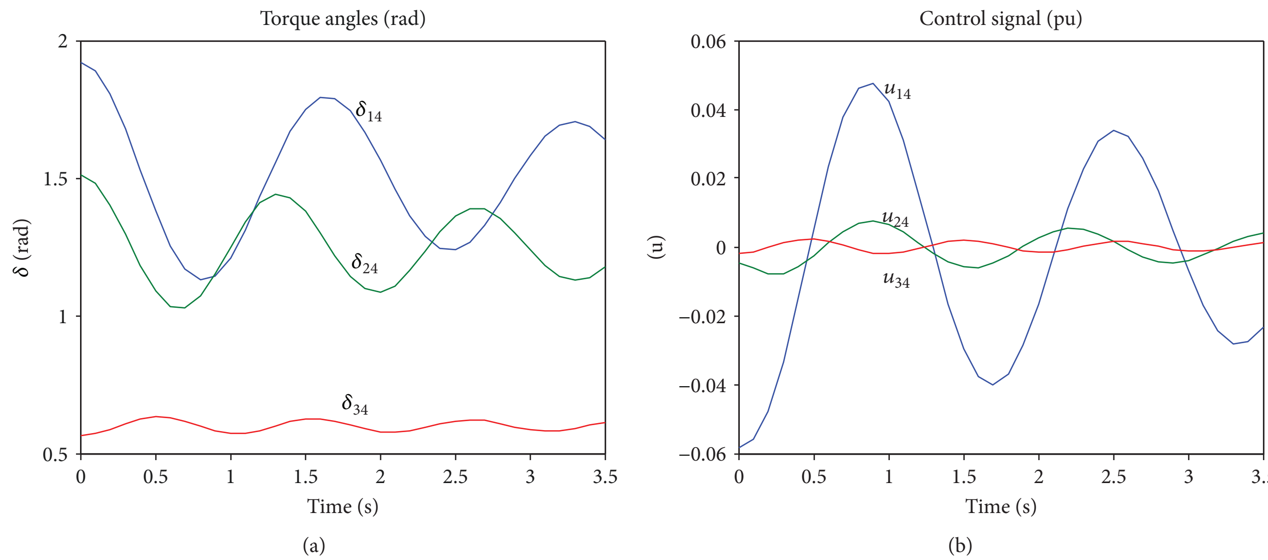

Figure 4: Rotor angle and control signals for decentralized H_∞ control: (a) rotor angle and (b) control signal.

7. Summary and Conclusion

(i) The paper presents a novel control technique for the stabilization of large power systems. The proposed controller satisfies the following constraints: (1) decentralized in using only the local states, (2) robust against system load variation, and (3) no violation of the control limits imposed in practice.

(ii) Since the proposed controller is in *state* feedback, it cannot be compared with the conventional PSS (CPSS), which is in *output* feedback. For future work, the ellipsoidal design for dynamic output feedback and comparison with CPSS will be conducted.

(iii) The large system is decomposed into subsystems, for each the effect on the rest of the whole system is considered as an external disturbance. The paper proposes a simple approach to rejection of the arbitrary-bounded external disturbances by means of the linear state feedback. It relies on the method of invariant ellipsoids, which reduces design of the optimal controller to the search of the least invariant ellipsoid of the closed-loop dynamic system. The concept of invariant ellipsoids allows restating the problem in terms of the linear matrix inequalities. Therefore, the controller design is reduced to the problems of semidefinite programming and one-dimensional convex minimization which readily yield to the numerical solution.

(iv) The effectiveness of the method was demonstrated by the stabilization of a typical multimachine system. Comparison with a commonly used, decentralized H_∞ controller shows the superiority of the proposed controller in swift damping out the rotor oscillations.

(v) The proposed decentralized saturated robust control is applied to a large system of 4-machine 11-bus system. The application of the proposed algorithm to larger systems is straight forward.

Appendix

The Multimachine Model

Consider generator number 4 as the reference. The multimachine model (30) and the norm-bounded matrices (31) and (32) for the system shown in Figure 1 are determined for each machine as follows:

(i) Machine number 1

$$\mathbf{A}_1 = \begin{bmatrix} 0 & 377 & 0 & 0 \\ -0.044064 & 0 & -0.088649 & 0 \\ -0.14338 & 0 & -0.3213 & 0.125 \\ 16063 & 0 & -1.189\times 10^5 & -1000 \end{bmatrix},$$
$$\mathbf{B}_1 = \begin{bmatrix} 0 & 0 & 0 & 2\times 10^5 \end{bmatrix}',$$
$$\mathbf{D}_1 = \begin{bmatrix} 0_{4\times 4} & \mathbf{A}_{12} & \mathbf{A}_{13} \end{bmatrix}, \tag{A.1}$$

where

$$\mathbf{A}_{12} = \begin{bmatrix} 0 & 0 & 0 & 0 \\ 0.044675 & 0 & -0.0047308 & 0 \\ 0.11323 & 0 & 0.099175 & 0 \\ 1883.6 & 0 & -66332 & 0 \end{bmatrix},$$
$$\mathbf{A}_{13} = \begin{bmatrix} 0 & 0 & 0 & 0 \\ -0.0029944 & 0 & -0.011401 & 0 \\ 0.0071248 & 0 & -0.0075558 & 0 \\ -8685 & 0 & -13491 & 0 \end{bmatrix}. \tag{A.2}$$

The norm-bounded matrices $\mathbf{M}_1, \mathbf{N}_1, \mathbf{F}_1$, and $\mathbf{H}_1$ associated with the uncertainties $\Delta\mathbf{A}_1$ and $\Delta\mathbf{D}_1$ are calculated as

$$\begin{aligned}
\mathbf{M}_1 &= \begin{bmatrix} 0 & -3.0914\times 10^{-5} & -1.2385\times 10^{-5} & -117.12 \end{bmatrix}',\\
\mathbf{N}_1 &= \begin{bmatrix} -79.141 & 0 & -24.385 & 0 \end{bmatrix},\\
\mathbf{F}_1 &= \begin{bmatrix} 0 & -6.2285\times 10^{-5} & -4.3476\times 10^{-5} & -127.42 \end{bmatrix}',\\
\mathbf{H}_1 &= \begin{bmatrix} -72.741 & 0 & -22.412 & 0 & 18.252 & 0 & 34.106 & 0 & 13.147 & 0 & -25.597 & 0 \end{bmatrix}.
\end{aligned} \tag{A.3}$$

(ii) Machine number 2

$$\begin{aligned}
\mathbf{A}_2 &= \begin{bmatrix} 0 & 377 & 0 & 0 \\ -0.061066 & 0 & -0.11197 & 0 \\ -0.15449 & 0 & -0.36443 & 0.125 \\ -2954 & 0 & -1.3221\times 10^{5} & -1000 \end{bmatrix},\\
\mathbf{B}_2 &= \begin{bmatrix} 0 & 0 & 0 & 2\times 10^{5} \end{bmatrix}',\\
\mathbf{D}_2 &= \begin{bmatrix} \mathbf{A}_{21} & 0_{4\times 4} & \mathbf{A}_{23} \end{bmatrix},
\end{aligned} \tag{A.4}$$

where

$$\begin{aligned}
\mathbf{A}_{21} &= \begin{bmatrix} 0 & 0 & 0 & 0 \\ 0.05652 & 0 & 0.023001 & 0 \\ 0.099968 & 0 & 0.12977 & 0 \\ 25431 & 0 & -40755 & 0 \end{bmatrix},\\
\mathbf{A}_{23} &= \begin{bmatrix} 0 & 0 & 0 & 0 \\ -0.0015434 & 0 & -0.011871 & 0 \\ 0.015892 & 0 & -0.001457 & 0 \\ -10868 & 0 & -17032 & 0 \end{bmatrix}.
\end{aligned} \tag{A.5}$$

The norm-bounded matrices $\mathbf{M}_2, \mathbf{N}_2, \mathbf{F}_2$, and $\mathbf{H}_2$ associated with the uncertainties $\Delta\mathbf{A}_2$ and $\Delta\mathbf{D}_2$ are calculated as

$$\begin{aligned}
\mathbf{M}_2 &= \begin{bmatrix} 0 & -1.088\times 10^{-4} & -2.0619\times 10^{-4} & -86.77 \end{bmatrix}',\\
\mathbf{N}_2 &= \begin{bmatrix} -52.649 & 0 & 31.505 & 0 \end{bmatrix},\\
\mathbf{F}_2 &= \begin{bmatrix} 0 & -1.0371\times 10^{-4} & -7.3511\times 10^{-5} & -105.53 \end{bmatrix}',\\
\mathbf{H}_2 &= \begin{bmatrix} -31.234 & 0 & -20.855 & 0 & -43.289 & 0 & 25.904 & 0 & 18.106 & 0 & 18.106 & 0 \end{bmatrix}.
\end{aligned} \tag{A.6}$$

(iii) Machine number 3

$$\begin{aligned}
\mathbf{A}_3 &= \begin{bmatrix} 0 & 377 & 0 & 0 \\ -0.092442 & 0 & -0.11741 & 0 \\ -0.19962 & 0 & -0.40745 & 0.125 \\ -18589 & 0 & -1.04\times 10^{5} & -1000 \end{bmatrix},\\
\mathbf{B}_3 &= \begin{bmatrix} 0 & 0 & 0 & 2\times 10^{5} \end{bmatrix}',\\
\mathbf{D}_3 &= \begin{bmatrix} \mathbf{A}_{31} & \mathbf{A}_{32} & 0_{4\times 4} \end{bmatrix},
\end{aligned} \tag{A.7}$$

where

$$\begin{aligned}
\mathbf{A}_{31} &= \begin{bmatrix} 0 & 0 & 0 & 0 \\ 0.010429 & 0 & 0.0027143 & 0 \\ 0.017504 & 0 & 0.016999 & 0 \\ 4930.1 & 0 & -6169.2 & 0 \end{bmatrix},\\
\mathbf{A}_{32} &= \begin{bmatrix} 0 & 0 & 0 & 0 \\ 0.0104 & 0 & -0.000296 & 0 \\ 0.023312 & 0 & 0.021148 & 0 \\ 1500 & 0 & -12862 & 0 \end{bmatrix}.
\end{aligned} \tag{A.8}$$

The norm-bounded matrices $\mathbf{M}_3, \mathbf{N}_3, \mathbf{F}_3$, and $\mathbf{H}_3$ associated with the uncertainties $\Delta\mathbf{A}_3$ and $\Delta\mathbf{D}_3$ are calculated as

$$\begin{aligned}
\mathbf{M}_3 &= \begin{bmatrix} 0 & -8.8747\times 10^{-5} & -4.3316\times 10^{-5} & -82.779 \end{bmatrix}',\\
\mathbf{N}_3 &= \begin{bmatrix} -57.851 & 0 & -8.9137 & 0 \end{bmatrix},\\
\mathbf{F}_3 &= \begin{bmatrix} 0 & -9.195\times 10^{-5} & 3.4393\times 10^{-5} & 83.395 \end{bmatrix}',\\
\mathbf{H}_3 &= \begin{bmatrix} -1.0784 & 0 & 8.2279 & 0 & -4.0578 & 0 & 4.041 & 0 & 57.424 & 0 & 8.8478 & 0 \end{bmatrix}.
\end{aligned} \tag{A.9}$$

Abbreviations

ANN:	Artificial neural networks
AVR:	Automatic voltage regulator
CPSS:	Conventional power system stabilizer
LMI:	Linear matrix inequality
LTI:	Linear time-invariant systems
PSS:	Power system stabilizer
$(^*)$:	In a matrix means the symmetric part
$(M+N+{}^*)$:	Means $(M+N+M' + N')$.

Nomenclature

$\Delta\delta_i$:	Torque angle of machine i, rad
$\Delta\omega_i$:	Speed deviation, pu
$\Delta E'_q$:	Deviation in the quadrature axis transient voltage of machine i, pu
$\Delta E_{f\,i}$:	Deviations in the field voltage of machine i, pu
$\mathbf{x}$:	The vector of the state variables
$\mathbf{u}$:	The vector of input variables
$\mathbf{A}$, $\mathbf{B}$, $\mathbf{D}$:	State, input, and disturbance matrices, respectively
$\mathbf{K}_i$:	The stabilizer gain of machine i
$\mathbf{w}(t)$:	Constrained disturbance
E:	Ellipsoid centered at the origin
$\mathbf{P}$:	Symmetric matrix of the ellipsoid
α, μ:	Constants
$\Delta\mathbf{w}_{ij}$:	Equal to $\Delta\mathbf{w}_i - \Delta\mathbf{w}_j$, pu.

Data Availability

The data used to support the findings of this study are available from the corresponding author upon request.

Conflicts of Interest

The authors declare that they have no conflicts of interest.

References

[1] P. Kundur, *Power System Stability and Control*, McGraw-Hill, 1994.

[2] P. W. Sauer, M. A. Pai, and J. H. Chow, *Power System Dynamics and Stability with Synchrophasor Measurement and Power System Toolbox*, J. Wiley, Second edition, 2018.

[3] N. Martins, "Efficient eigenvalue and frequency response methods applied to power system small-signal stability studies," *IEEE Transactions on Power Systems*, vol. 1, no. 1, pp. 217–224, 1986.

[4] B. Pal and B. Chaudhuri, *Robust Control in Power Systems*, Springer, 1st edition, 2005.

[5] H. M. Soliman, A. L. Elshafei, A. A. Shaltout, and M. F. Morsi, "Robust power system stabilizer," *IEE Proceedings - Generation, Transmission and Distribution*, vol. 147, no. 5, pp. 285–291, 2000.

[6] C. Zhu, M. Khammash, V. Vittal, and W. Qiu, "Robust power system stabilizer design using H_∞ shaping approach," *IEEE Transactions on Power Systems*, vol. 18, no. 2, pp. 810–818, 2003.

[7] K.-Z. Liu and Y. Yao, *Robust Control Theory and Applications*, Wiley, 2016.

[8] H. M. Soliman, "Resilient observer-based power system stabilizers," *Transactions of the Institute of Measurement and Control*, vol. 38, no. 8, pp. 981–991, 2016.

[9] T. Hussein, M. S. Saad, A. L. Elshafei, and A. Bahgat, "Damping inter-area modes of oscillation using an adaptive fuzzy power system stabilizer," *Electric Power Systems Research*, vol. 80, no. 12, pp. 1428–1436, 2010.

[10] G. K. Dill and A. S. e Silva, "Robust design of power system controllers based on optimization of pseudospectral functions," *IEEE Transactions on Power Systems*, vol. 28, no. 2, pp. 1756–1765, 2012.

[11] W. Peres, J. A. Passos Filho, and I. C. da Silva Jr., "Coordinated tuning of power system stabilizers using bio-inspired algorithms," *International Journal of Electrical Power & Energy Systems*, vol. 64, pp. 419–428, 2015.

[12] S. M. A. Elazim and E. S. Ali, "Optimal power system stabilizers design via cuckoo search algorithm," *International Journal of Electrical Power & Energy Systems*, vol. 75, pp. 99–107, 2016.

[13] S. M. A. Elazim and E. S. Ali, "Optimal SSSC design for damping power systems oscillations via gravitational search algorithm," *International Journal of Electrical Power & Energy Systems*, vol. 82, pp. 161–168, 2016.

[14] P. Jagadeesh and M. Sai Veerraju, "Particle swarm optimization based power system stabilizer for SMIB system," in *2016 International Conference on Emerging Trends in Engineering, Technology and Science (ICETETS)*, pp. 1–6, Pudukkottai, India, February 2016.

[15] E. S. Ali and S. M. Abd-Elazim, "Coordinated design of PSSs and TCSC via bacterial swarm optimization algorithm in a multimachine power system," *International Journal of Electrical Power & Energy Systems*, vol. 36, no. 1, pp. 84–92, 2012.

[16] M. R. Shakarami and I. F. Davoudkhani, "Wide-area power system stabilizer design based on grey wolf optimization algorithm considering the time delay," *Electric Power Systems Research*, vol. 133, pp. 149–159, 2016.

[17] A. Khodabakhshian, M. R. Esmaili, and M. Bornapour, "Optimal coordinated design of UPFC and PSS for improving power system performance by using multiobjective water cycle algorithm," *International Journal of Electrical Power & Energy Systems*, vol. 83, pp. 124–133, 2016.

[18] H. Xin, D. Gan, T. S. Chung, and J. Qiu, "A method for evaluating the performance of PSS with saturated input," *Electric Power Systems Research*, vol. 77, no. 10, pp. 1284–1291, 2007.

[19] H. M. Soliman and H. A. Yousef, "Saturated robust power system stabilizers," *International Journal of Electrical Power & Energy Systems*, vol. 73, pp. 608–614, 2015.

[20] H. M. Soliman and K. El Metwally, "Robust pole placement for power systems using two-dimensional membership fuzzy constrained controllers," *IET Generation, Transmission & Distribution*, vol. 11, no. 16, pp. 3966–3973, 2017.

[21] S. Tarbouriech, G. Garcia, J. M. Gomes da Silva Jr., and I. Queinnec, *Stability and Stabilization of Linear Systems with Saturating Actuators*, Springer, London, 2011.

[22] A. Benzaouia, F. Mesquine, and M. Benhayoun, "Saturated control of linear systems," in *Studies in Systems, Decision and Control*, Springer, Cham, 2018.

[23] M. A. Dahleh and I. J. Diaz-Bobillo, *Control of Uncertain Systems: A Linear Programming Approach*, Prentice Hall, Englewoods Cliffs, NJ, USA, 1995.

[24] Z. Lin and A. Saberi, “Semi global exponential stabilization of linear discrete time systems subject to input saturation via linear feedbacks,” *Systems & Control Letters*, vol. 24, no. 2, pp. 125–132, 1995.

[25] D. Li, Y. Xi, and F. Gao, “Synthesis of dynamic output feedback RMPC with saturated inputs,” *Automatica*, vol. 49, no. 4, pp. 949–954, 2013.

[26] V. Bandal and B. Bandyopadhyay, “Robust decentralised output feedback sliding mode control technique-based power system stabiliser (PSS) for multimachine power system,” *IET Control Theory & Applications*, vol. 1, no. 5, pp. 1512–1522, 2007.

[27] A. Kumar, “Power system stabilizers design for multimachine power systems using local measurements,” *IEEE Transactions on Power Systems*, vol. 31, no. 3, pp. 2163–2171, 2016.

[28] G. Gurrala and I. Sen, “Power system stabilizers design for interconnected power systems,” *IEEE Transactions on Power Systems*, vol. 25, no. 2, pp. 1042–1051, 2010.

[29] W. Qiu, V. Vittal, and M. Khammash, “Decentralized power system stabilizer design using linear parameter varying approach,” *IEEE Transactions on Power Systems*, vol. 19, no. 4, pp. 1951–1960, 2004.

[30] F. Blanchini, “Set invariance in control,” *Automatica*, vol. 35, no. 11, pp. 1747–1767, 1999.

[31] S. A. Nazin, B. T. Polyak, and M. V. Topunov, “Rejection of bounded exogenous disturbances by the method of invariant ellipsoids,” *Automation and Remote Control*, vol. 68, no. 3, pp. 467–486, 2007.

[32] I. Erceg, D. Sumina, S. Tusun, and M. Kutija, “Power system stabilizer based on pointwise min-norm control law,” *Electric Power Systems Research*, vol. 143, pp. 215–224, 2017.

[33] H. Werner, P. Korba, and T. C. Yang, “Robust tuning of power system stabilizers using LMI-techniques,” *IEEE Transactions on Control Systems Technology*, vol. 11, no. 1, pp. 147–152, 2003.

[34] G. R. Duan and H. H. Yu, *LMIs in Control Systems: Analysis, Design and Applications*, CRC Press, Boca Raton, 1st edition, 2013.

[35] K. Tang and G. K. Venayagamoorthy, “Damping inter-area oscillations using virtual generator based power system stabilizer,” *Electric Power Systems Research*, vol. 129, pp. 126–141, 2015.

[36] S. Khosravani, I. N. Moghaddam, A. Afshar, and M. Karrari, “Wide-area measurement-based fault tolerant control of power system during sensor failure,” *Electric Power Systems Research*, vol. 137, pp. 66–75, 2016.

[37] K. Tang and G. K. Venayagamoorthy, “Adaptive inter-area oscillation damping controller for multi-machine power systems,” *Electric Power Systems Research*, vol. 134, pp. 105–113, 2016.